Journal of Civil Structural Health Monitoring
https://doi.org/10.1007/s13349-022-00628-7

ORIGINAL PAPER

Structural assessment of the pedestrian bridge accessing Civita di Bagnoregio, Italy

Giacomo Buffarini[1] · Paolo Clemente[1] · Sonia Giovinazzi[1] · Chiara Ormando[2] · Federico Scafati[3]

Received: 26 May 2022 / Accepted: 26 August 2022

Abstract
The paper presents the results of the vibration tests carried out on the pedestrian bridge accessing Civita di Bagnoregio, Italy. The structure was in bad health condition. The external beams were damaged due to deterioration exacerbated by the combined actions of rain and wind. The circular piers were also damaged with several cracks where the concrete cover was spliced and the reinforcement bars were exposed. The analysis presented in the paper focuses on the highest five piers, which seemed to show an irregular behavior during a preliminary experimental campaign. The results of the experimental campaign presented in this paper showed that the structural behavior of the bridge was qualitatively similar to the expected one. The reduced stiffness, due to the observed widespread damage state, amplified the vibrations uniformly along the structure. The Italian Guidelines for the risk and safety assessment of bridges and viaducts, issued in 2020, have been applied and tested in this study and the results are presented in the paper.

Keywords Structural health monitoring · Pedestrian bridges · Experimental analysis · Experimental dynamic analysis · Risk and safety assessment of bridges

1 Introduction

The bridge and viaduct heritage is at risk all over the world. After the 1950s and 1960s, when several structures were built, bridge and viaduct that have been operational for several decades began to show the signs of time, exacerbated by the lack of adequate maintenance. Nowadays, in Italy and all over the world, there are bridges made of different materials, i.e., masonry, reinforced concrete and steel, older than 50 years. Several of them have been designed and built according to design standards very different from the current ones, where the moving loads accounted for were much lower than the ones considered by the current design standards and, above all, where seismic actions were either neglected or much lower than the ones known and considered nowadays [1].

The safeguarding of these infrastructures is urgent and imperative. Their lifetime should be extended as much as possible, guarantying on the meantime the current safety standards at the fullest possible extent. An appropriate maintenance program is required aiming to avoid the occurrence of serious irreversible damage and to reduce maintenance costs by acting through preventive maintenance [2–4].

✉ Paolo Clemente
paolo.clemente@enea.it

Giacomo Buffarini
giacomo.buffarini@enea.it

Sonia Giovinazzi
sonia.giovinazzi@enea.it

Chiara Ormando
chiara.ormando@uniroma2.it

Federico Scafati
federico.scafati@guest.univaq.it

[1] ENEA, Italian National Agency for New Technologies, Energy and Sustainable Economic Development, Casaccia Research Centre, Via Anguillarese 301, 00123 Rome, Italy

[2] University of Tor Vergata, Via Politecnico 1, 00133 Rome, Italy

[3] Department of Civil, Construction-Architectural and Environmental Engineering, University of L'Aquila, Piazzale Ernesto Pontieri 1, Monteluco Di Roio, 67100 L'Aquila, Italy

Published online: 13 September 2022

Some countries have made exceptional efforts to promote the maintenance and preservation of bridges and viaducts. The USA developed an extensive regulatory framework on the subject. In 1971, the *National Bridge Inspection Standards* (NBIS) were released, defining, for the first time in the country, frequency and modality of visual inspection and the professional requirements of the inspectors. In the same year, the *National Bridge Inventory* was established. At the beginning of the 70s, other manuals and guidelines were released by the *American Association of State Highway and Transportation Officials* (AASHTO) and the *Federal Highway Administration* (FHWA) to regulate the maintenance and the appraisal of bridges and viaducts. These aforementioned standards and manuals have been updated, modified and replaced several times. The last update of the NBIS was in 2009.

In Europe, Great Britain is very advanced in the maintenance of bridges and viaducts thanks to a fifteen-year program launched in 1987 to evaluate bridges and viaducts of the main road networks aiming to adapt them to the moving loads considered by the current design standards.

In Italy, the first standard ruling bridge maintenance was released in 1967 [5]; the standard summarily defined the main steps of a correct maintenance and identified the practitioners entitled to preserve these structures. Further guidelines were released during the years, and in 2001, a national bridge inventory was established. After the release of OPCM 3274 in 2003 [6], the Italian Department of Civil Protection proposed and issued two survey forms for the survey and seismic assessment of all the strategic bridges in Italy; only in 2008, an entire chapter of the New Technical Code (NTC-2008) [7], was dedicated to the safety evaluation and retrofitting of existing structures, including bridges. The NTC-2008 was updated in 2018 becoming NTC-2018 [8]. Finally, in 2020, the Italian Ministry for Infrastructure and Transports released the new "*Guidelines for Risk Classification, Risk Management, Safety Evaluation and Monitoring of Existing Bridges*" (LG2020) [9] defining a detailed operative framework for the structural appraisal of bridges and viaducts based on a multilevel approach including six different Levels of analysis, from L0 to L5, in increasing order of accuracy and complexity of analysis. The application of the first three levels, i.e., L0, L1, L2, leads to the definition of a Class of Attention of the bridge (CA) via a simple and expeditious evaluation of the bridge health status, based on census data and visual inspections. The LG2020 includes 5 different CAs, namely: Low, Low-Medium, Medium, Medium–High and High. L3 and L4 are applied only in case a bridge has a Medium or Medium High CA and a High CA, respectively. L5 is applied only if the structure is a strategic bridge, using sophisticated analysis.

Still nowadays visual inspections are the main way for inspecting bridges and viaducts, although they imply several issues. Visual inspections require long times and excessive costs and, above all, should be entrusted to technicians of great competence and experience. Furthermore, inspections are always very subjective: a recent American study showed that the results of inspections have a great deal of variability, especially in the synthetic final judgment. Moreover, detailed inspections, not always possible because of the scarce funding available, are unlikely to detect defects further to the ones already detectable during routine inspections [10, 11].

The alternative to visual inspections is structural health monitoring (SHM), which can allow keeping a large number of bridges under control with a lower effort both in terms of time and cost [12–14]. This can be coupled with seismic monitoring to analyze the current behavior under traveling and seismic actions, allowing to define the dynamic properties of the structure with different techniques [15–18]. Until now, several bridges were permanently or temporarily equipped with a structural monitoring system [19–23]. However, the goal to be pursued should be an exponential increase of the permanent structural monitoring of existing bridges and viaducts; this can strongly support the reduction of maintenance costs with an increase in reliability, thanks to the reduction of inspection costs, but also to the increase in preventive maintenance, which is less expensive than on-demand maintenance [24–27].

While aiming and waiting for a widespread monitoring on the bridge and viaduct portfolio in Italy, the periodic experimental analysis on materials and structures can represent a valid alternative to contribute to the assessments of the current status of the health at single-bridge level by updating and validating the mathematical model [28–31]. At national scale level, the final goal should be the assessment and evaluation of all the portfolio via performance indicators [32, 33] and also by the collection and collation of all the data relevant for characterizing the physical and functional performance of bridges and viaducts in a suitable standardized and interoperable platform, also able to perform preliminary elaborations [34].

In this paper, the procedure of the LG2020 is implemented to analyze the structural health status of the pedestrian bridge at Civita di Bagnoregio. Since the resulting CA was "High", the bridge was analyzed in detail. Based on the experimental campaigns on materials and the experimental vibrational analysis, carried out in 1997 when the bridge showed high amplitude vibrations under the wind action, a numerical model of the structure was set up and a vulnerability analysis was performed.

The paper is organized as follows. After a brief description of the bridge, based on the census and a suitable structural relief, the results of the visual inspections are presented, and the CA is evaluated. Then the results of the experimental analyses are reported and, finally, a finite element model is set up and used for the seismic safety check.

2 The site and the structure

Civita di Bagnoregio, Lazio Region, Italy, is well-known worldwide as the "dying town" [35] because of its progressive population reduction and decay due to a series of natural disaster, especially landslides and earthquakes. Furthermore, relevant unsettlement movements have occurred since the twentieth century. It is a small town of Etruscan origin, placed on the top of a tuff hill, 443 m *asl* and 250 m above the bottom of the surrounding valley. It is connected to Bagnoregio, the main part of the municipality, by means of a pedestrian bridge running over a narrow saddle (Fig. 1). The town was a vital center during the early Middle Ages, but for 200 years, no new buildings have been constructed.

The disasters also affected the bridge, which was rebuilt several times after the first known collapse in 1684. The earthquake of June 11, 1695 caused the failure of the bridge and also the death of 32 people. In 1759 and 1764, landslides caused the collapse of the bridge again. Following the continuous interruptions of the access to Civita, in 1810, the evacuation of the town was decided, but the 400 inhabitants opposed this decision. Several unsettlement movements occurred in the twentieth century; in 1944, the existing masonry arch bridge was destroyed by the retreating German troops. After the Second World War, the damaged part of the bridge was substituted by a wooden footbridge, which collapsed in 1963 with the under-scarp wall. Then a new pre-stressed concrete bridge was built and completed in September 1965. Before its inauguration, the structure collapsed at its anchorage point on the Civita side and was temporarily substituted by a steel bridge.

The present bridge comprises 14 spans, each one of them simply supported on the piers (Fig. 2), spaced approximately 19.00 m. Starting from Civita, five spans are located on a 20% gradient downhill. The heights of the piers from pier 1 to pier 5 vary from 11 to 15 m, pier 4 being the highest. The bridge between pier 5 and pier 9 is almost horizontal. The last part, from pier 9 to pier 13, is uphill with a 6% gradient. Piers from 6 to 13 are much shorter than the others.

Fig. 2 View of the bridge

Each deck is composed of three pre-stressed concrete beams and a concrete slab, exception for the first one starting from Civita, which has five beams. The total height of the cross-section is 80 cm (65 + 15). The horizontal center distance between the beams is 90 cm, and the width of the bridge is 2.50 m (4.00 m for the first span from Civita), including the two longitudinal parapets (Fig. 3). Each span has a length of about 16.70 m, but the first one is 16.00 m. The beams rest on lead pads, placed at the top of the piers.

The piers from 1 to 9 are composed of 4 circular columns, whose diameter is 50 cm, an upper plate of 3.25 m in the longitudinal direction and of 2.80 m in the transversal one, and 0.65 m height. The piers from 10 to 13 have only two columns and a pier cap of 1.00 × 2.80 m. The columns start from a foundation plinth (or pile cap), supported by concrete

Fig. 1 Global view of the bridge (Civita is on the left)

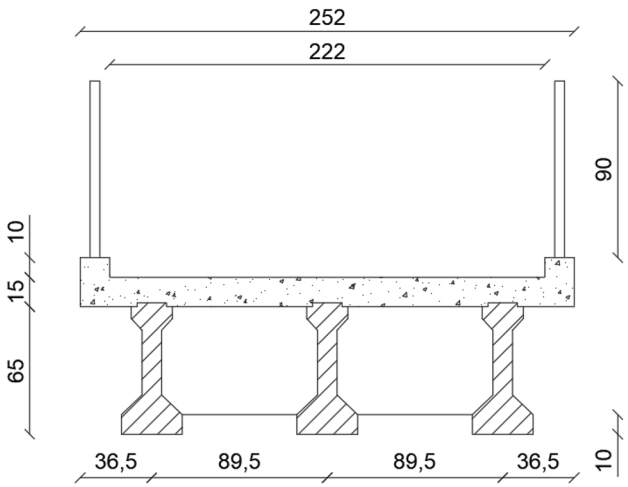

Fig. 3 Cross section of the deck (dimensions in cm)

piles with length variable from 10 m, for the shortest piers, to 25 m for the tallest ones.

3 Visual inspection and class of attention

A visual inspection of the bridge was conducted as the first step for implementing the risk and safety assessment according to LG2020.

At the time of the inspection, most of the structural elements were in bad condition, because of different issues, including: corrosion of the reinforcing steel; spalling of the concrete; and carbonation of the concrete in some elements. The effects were particularly evident for the external beams, where the combined action of rain and wind was favored by the presence of short water drain hoses (Fig. 4). Steel reinforcing bars were also exposed at the zone close to the bearings (Fig. 5).

Several vertical cracks could be seen in the columns, where the concrete cover was split, and the reinforcement bars were discovered. The upper plates of the piers were damaged too. Finally, the lead pads, placed at the top of the piers appeared very flat between the beams and the pier top and could no longer allow the elasticity rotations of the beams.

The level of defects was certainly high. However, it was believed that these defects could not affect the stability of the bridge immediately, thanks to the good status of the central beam, which was almost intact being protected by the two external ones. This was confirmed by the experimental tests described in the next section.

According to the LG2020, four types of risks must be considered: (1) structural/foundation; (2) seismic; (3) landslide; and (4) hydraulic risks. For each one of them, a Class of Attention (CA) is defined by combining the assessed level of hazard, vulnerability and exposure. A combination of these CAs allows defining the global CA as detailed in the following paragraphs.

Fig. 4 The carbonation of the concrete and the reinforcing bar exposed

Fig. 5 Reinforcing bar exposed in proximity of the support

With reference to the structural/foundation risk, the structural hazard, related to admissible load on the bridge and the daily number of heavy vehicle passages for each lane, can be assumed to be low (L). Instead, the vulnerability class is certainly high (H) because so is the level of defects, independently of the other parameters (design code, structural type and span, period of construction). The exposure, related to the daily number of total passages, the span, the presence of alternative roads, the transport of high-risk goods and the type of structure over crossed, is low (L). Due to the high vulnerability, the structural/foundation CA class is high (H) despite the low hazard and exposure.

With reference to the seismic risk, the value of the horizontal acceleration on rigid soil for a probability of exceedance of 10% in 50 years, is $a_g = 0.144$ g, while the topography type is T4, according to NTC-2018 classification (a smaller width crest and inclination > 30°). The ground being of type A according to NTC-2018 classification, the seismic hazard CA is medium–high (MH). The vulnerability, which depends on the structural type, material, number of spans,

Table 1 Classes of Attention for the different risks

Risk	Hazard/susceptibility	Vulnerability	Exposure	CA
Structural/foundation	Low	High	Low	High
Seismic	Medium–High	High	Low	High
Landslide	Medium–High	High	Low	Medium–High
Hydraulic	–	–	–	Low
Global CA				High

span length, seismic design and defects, is high (H), mainly because of the severe level of defects. The exposure is low (L), as for the structural/foundation risk. The final seismic CA is high (H).

The landslide susceptibility depends on the present situation (active or potential), the speed and the magnitude, i.e., the volume, the presence of mitigation interventions and the reliability of the evaluation. In this case, the landslide susceptibility CA is medium (MH). Considering the structural and foundation types and the interference with the bridge, the vulnerability CA is high (H). The exposure CA is low (L), as for the seismic risk. The global landslide CA is medium–high (MH).

Finally, the hydraulic risk can be considered negligible, and the corresponding CA is low (L). The combined landslide and hydraulic CA is medium (M).

The global CA is high (H). The values of the different partial CAs and the final ones are reported in Table 1.

4 Experimental analyses

When the global CA is high (H) as resulted for the pedestrian bridge accessing Civita di Bagnoregio, (Table 1), the LG2020 requires a detailed analysis of the bridge including experimental analysis and mathematical modeling. The experimental analysis encompassing, soil tests, material tests, static load and impulse tests as well experimental dynamic analysis are extensively described in the following paragraphs.

4.1 Soil tests

Previous laboratory analyses on disturbed and undisturbed soil samples, were carried out by ENEA [36], at different depths, and pointed out that the ground is mainly composed of weakly over-consolidated clayey silts. These silts have mechanical characteristics typical of the Plio-Pleistocene clays, with a friction angle of about 30° and an undrained cohesion higher than 0.2 N/mm^2.

Three cone penetration tests (CPT), having depths of 17.8, 18.6 and 16.8 m, respectively, were performed by SGM Srl [37]. Furthermore, a standard dynamic test (DPHS) was performed at the lowest location along the saddle. The outcomes confirmed the results of the previous investigations performed by ENEA and were used to evaluate the load carrying capacity of the piles. The limit load varies from 7.5 to 10 MN for a length of 10 m, and from 11 to 14 MN for a length of 20 m. These turned out to be much higher than the maximum loads on each pile at the ultimate limit state (< 500 kN), evaluated by means of the numerical model described in the next paragraph.

Table 2 Number of tests for each element type

Element	Ultrasonic	Sclerometer	Pull-out	Carbonation
Beams	72	720	36	36
Pier columns	50	560	33	33
Foundations	24	240	12	11
Total	146	1520	81	80

Table 3 Minimum and maximum carbonation depths (mm)

Element	Min	Max
Deck of span 6	2.5	3.1
Pier 2	12.0	15.0
Foundation pier 6	2.4	3.5

4.2 Material tests

Ultrasonic tests, sclerometer tests, pull-out tests and carbonation tests were carried out on the beams, piers and foundation plinths as synthesized in Table 2 [37].

Pacometric tests on the columns of the piers allowed to identify the presence of vertical bars (10 ϕ 14) and stirrups

Table 4 Average values measured with the tests

Element	Pull-out (N/mm^2)	Ultrasonic (m/s)	Sclerometer (N/mm^2)
Beams	49.0	3023	44.9
Pier columns	34.2	2553	34.2
Foundations	22.8	2391	23.5

Table 5 Average values of the concrete and steel strength

Element	Cubic strength (N/mm^2)	Steel (N/mm^2)
Beams	48.9	535
Pier columns	33.5	535
Foundations	28.0	399

(ϕ 6/15 cm). Finally, endoscopic tests on the columns of the piers 3 and 4 by radial holes, allowed to check an external coating whose thickness was 150 mm with better characteristics than the internal portion, and to detect the absence of defects in the internal portion.

With reference to the carbonation tests, pull-out cones were used. In Table 3, the minimum and maximum values of the carbonation depth for the most affected elements are reported.

The average strength values of the results are reported in Table 4. The tests pointed out the good degree of homogeneity of the concrete for each set of structural elements (beams, piers and foundations).

Laboratory compression tests were carried out on 10 concrete specimens. The average compression strengths were very similar to those obtained from the non-destructive tests.

Table 6 Deflections during the static tests

Test	Force (kN)	Displacement (mm)
1	140	6.55
2	144	6.40
3	146	6.54
4	146	6.70
5	148	5.80

Table 5 also reports the breaking stresses of the steel reinforcing bars.

4.3 Static load and impulse tests

Static load tests were carried out on five spans. A concentrated load, equivalent to the distributed one and measured by a load cell, was applied in the middle of the span using a contrast beam, as shown in Fig. 6. The force was produced using two hydraulic pull jacks, anchored to the columns of the adjacent piers. The deflections were measured by means of five inductive transducers. The results are summarized in Table 6. The measured values were much lower than the theoretical ones, obtained for a simply supported beam of span $L = 16.80$ m and moment of inertia $I_x = 1.07 \cdot 10^4$ m^4. In all the tests, a negligible deviation from the theoretical linear behavior and a negligible residual displacement were detected.

Dynamic tests using an impulse due to a mass of 1.0 kg dropped on the deck from 1.5 m were performed. The first vertical frequency of spans 1–5 is reported in Table 7. The results were very similar to those obtained during ambient vibration tests and the passage of a 6.0 kN vehicle.

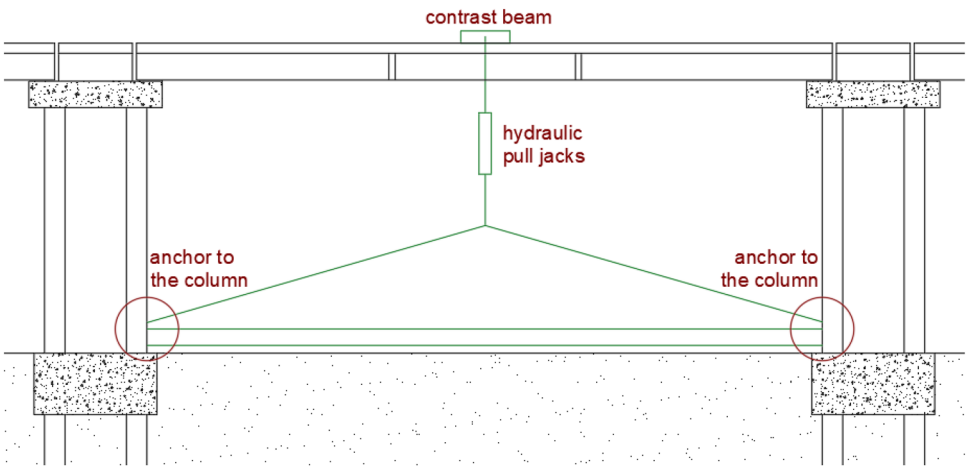

Fig. 6 Scheme of the static load tests

Fig. 7 The tallest part of the viaduct, from piers 1 to pier 5

In conclusion, despite of the described bad conditions of the bridge, the static analyses showed a quite uniform and good performance of the girders. This occurrence demonstrated that damage interests only the external surface; therefore, the structure could be successfully repaired by means of usual repair strategies. The experimental campaign carried out by ENEA targeted exclusively the dynamic behavior of the bridge in the transversal and longitudinal directions. The portion of the viaduct from pier 1 to pier 5 was tested in detail (Fig. 7). The results are discussed in the following paragraph.

4.4 Experimental dynamic analysis

The experimental set-up was composed of eight seismometers Kinemetrix SS1 (Fig. 8a, b) connected by cables to a signal conditioner. The signals recorded by the eight seismometers, used in a synchronized way, were collected and analyzed in real-time to have control of the experimental results in real-time.

Sensors were deployed in several configurations. Five time-histories lasting 64 s were recorded for each configuration, with a sampling rate of 128 Hz. This was done to show the repeatability of the vibrational characteristics and to get average values of the characteristics. Both ambient and

(a)

(b)

Fig. 8 Seismometer deployed (**a**) at the basement and (**b**) at the top of a pier

forced vibrations were considered, the latest being caused by the passage of pedestrians or vehicles of small size.

The recorded data were analyzed in the time domain, to find out the peak values, and in the frequency domain, plotting the power spectral density (*PSD*) of each record and the cross-spectral density (*CSD*) for each couple of records, with the corresponding phase factor and coherence function.

As already mentioned, the behavior of the viaduct was analyzed with particular focus on its portion between pier 1 and pier 5. In the configurations used in the present analysis, velocimeters were deployed at the locations shown in Fig. 9, at the top and the pile caps of piers 1, 2, 3 and 5, first in the transversal and then in the longitudinal direction.

Under ambient vibrations, velocity peak values lower than 0.02 mm/s were recorded at the pier base in the

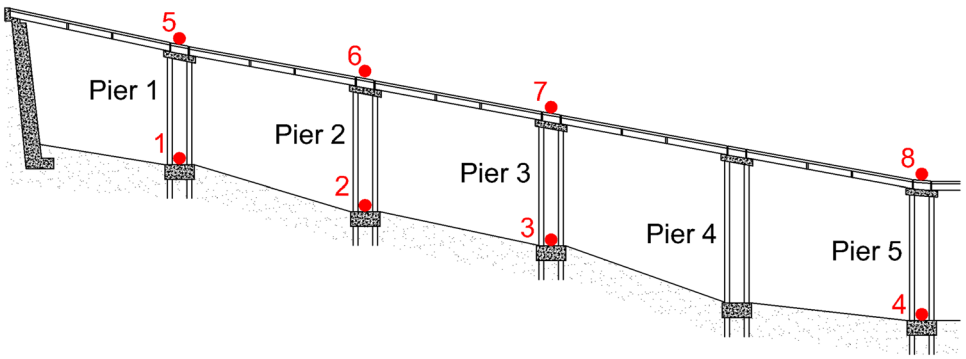

Fig. 9 Sensor deployments to analyze the global behavior of the tallest part of the viaduct

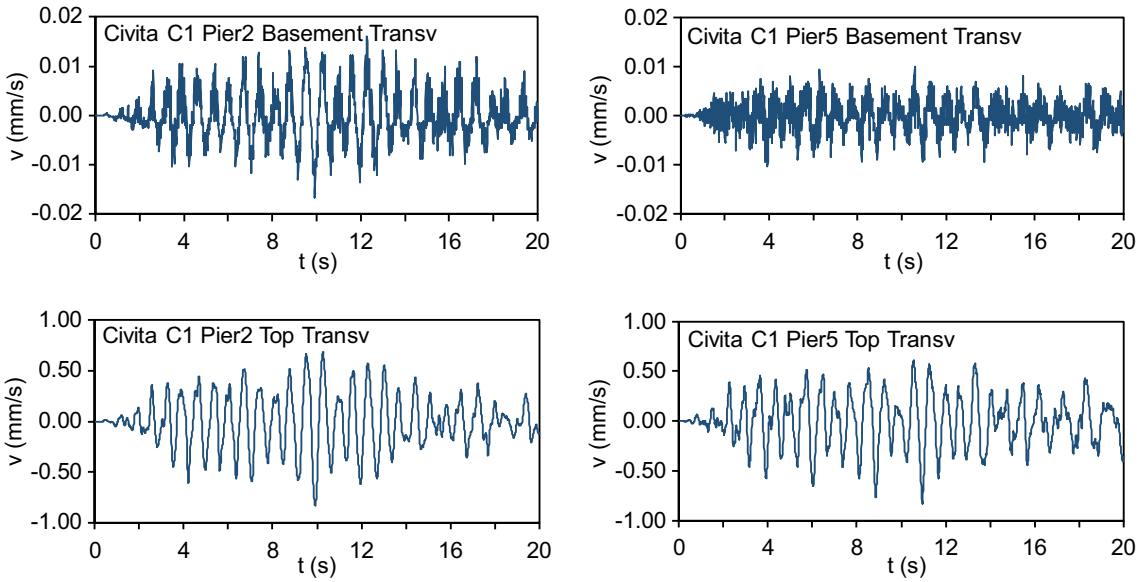

Fig. 10 Time histories at the basements and the tops of pier 2 and pier 5 in the transversal direction, under ambient vibrations

Table 7 Vertical frequencies of the first five spans

Span	Freq. (Hz)
1 (5 beams)	11.3
2	8.8
3	6.3
4	6.3
5	6.7

Table 8 Experimental and numerical resonance frequencies in the transversal direction

Freq (Hz)	Exp. Freq. (Hz)	Num. Freq. (Hz)
f_1	0.95	0.95
f_2	1.38	1.43
f_3	2.07	2.14
f_4	2.83	2.95

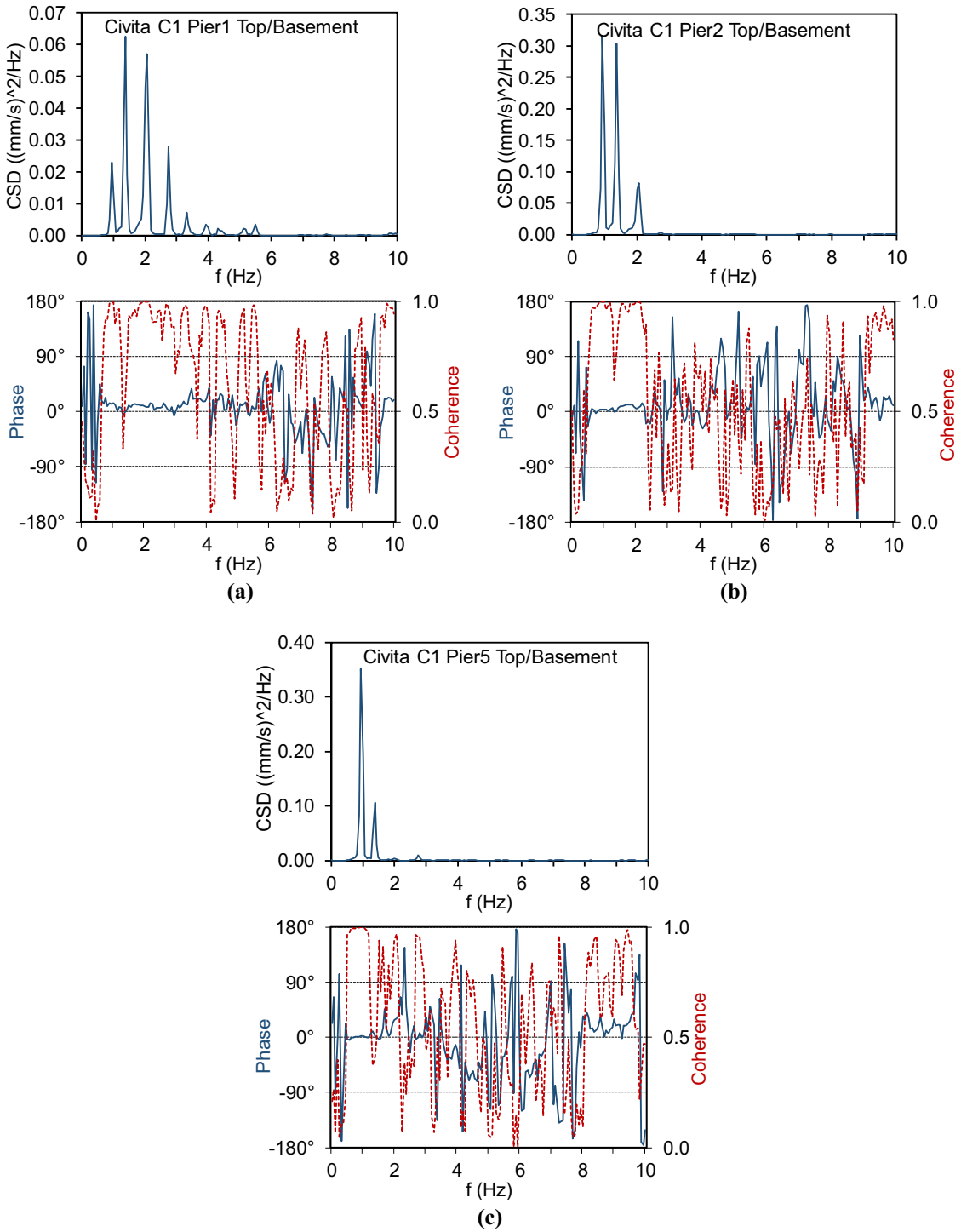

Fig. 11 CSDs of recordings at the top and the basement of **a** Pier 1, **b** Pier 2 and **c** Pier 5, in the transversal direction, under ambient vibrations

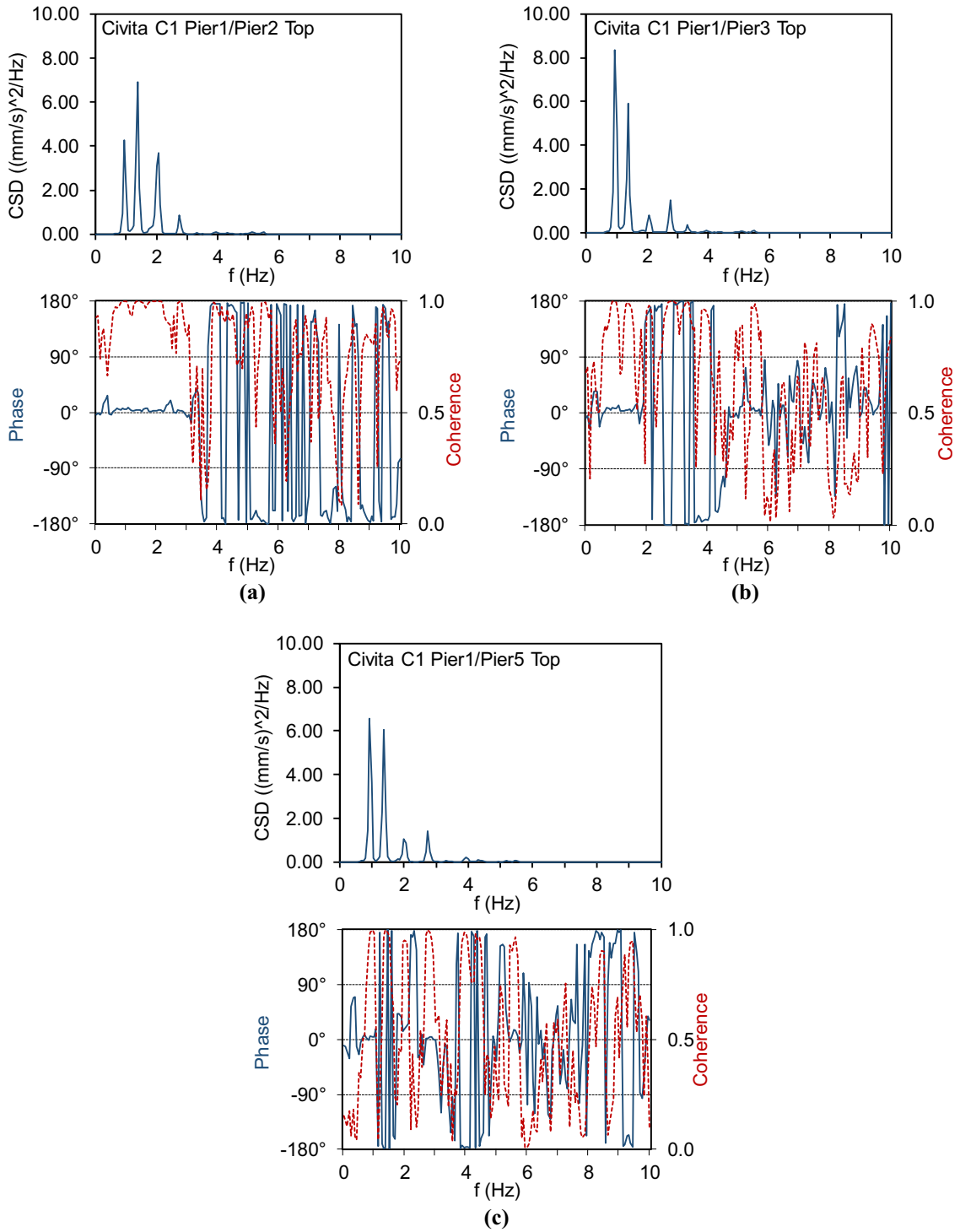

Fig. 12 CSDs of recordings in the transversal direction, under ambient vibrations, of **a** the tops of Pier 1 and Pier5, **b** Pier 1 and Pier 3 and **c** Pier 1 and Pier 5

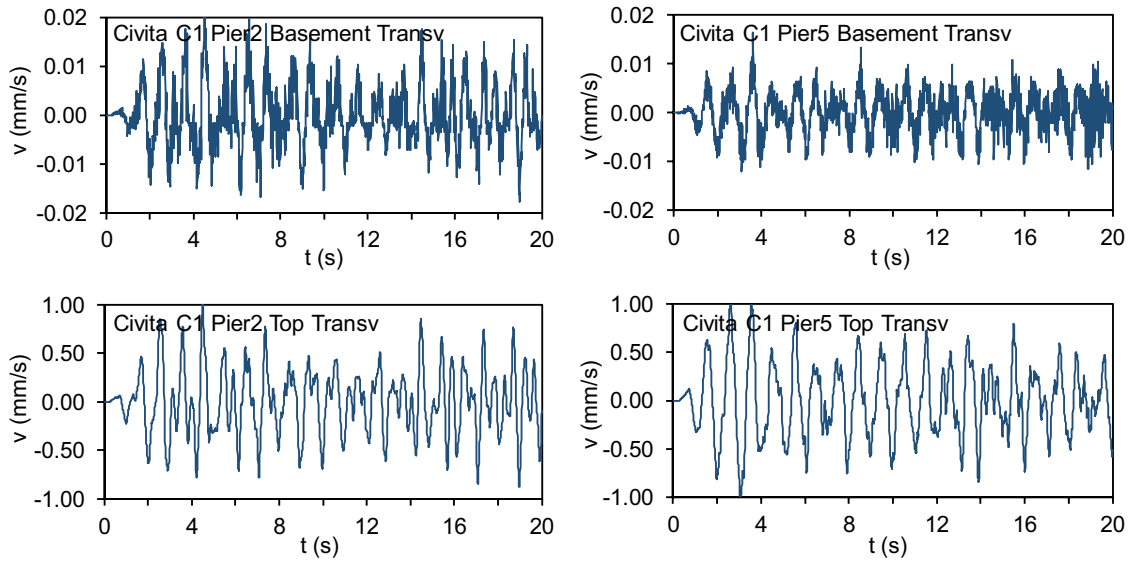

Fig. 13 Time histories at the basements and the tops of piers 2 and 5, in the longitudinal direction, under forced vibrations (C1)

transversal direction (Fig. 10), while values between 0.40 and 1.00 mm/s were recorded at the pier tops in the same direction. In Fig. 11, the cross-spectral densities between sensors at the pile cap and sensors at the top of piers 1, 2 and 5, respectively, are plotted. The resonance frequencies listed in Table 8 are particularly apparent in all the spectra. This occurrence demonstrated that the viaduct behaved as a whole. The cross-analysis between the records at different piers confirmed this result. In more detail, for each pier, the record at the base was in phase with the corresponding record at the top, at all the resonance frequencies. Peaks at the same frequencies are also apparent in all the cross-spectra between the sensors at the tops of the different piers, with significant values of the phase factor and the coherence function (Fig. 12).

During the passage of groups of pedestrians (forced vibrations), velocity peaks at the pile caps were lower than 0.03 mm/*s*, while the maximum velocities at the tops were between 0.5 and 1.5 mm/*s* (Fig. 13). In both cases, the amplification factors were between 20 and 50. The cross-spectra analysis confirmed the dynamic behavior of the bridge found under ambient vibrations (Figs. 14 and 15).

The analysis of the phase factors allowed to find out the modal shapes associated with the resonance frequencies (Fig. 16). We concluded that the girder behaved as a beam supported by horizontal elastic restraints at the piers.

In the longitudinal direction, ambient vibrations with velocity peaks values equal to 0.005 mm/*s* were recorded at the pile cap and 0.03 mm/s at the tops, with an amplification factor equal to 6. During the passage of people, peaks up to 0.05 mm/s and 0.15 mm/s were recorded at the pile cap and the tops, respectively. The analysis in the frequency domain pointed out the same resonance frequencies of the transversal direction but also at higher frequencies between 4.5 and 8.5 Hz. The spectral amplitudes were very low compared to those of the records in the transversal direction.

In other configurations, not shown here, sensors 4 and 8 were at the pile cap and at the top of pier 4, respectively, obtaining the same results about the behavior of the bridge.

The dynamic behavior of each pier was analyzed in detail, deploying the sensors as in Fig. 17. Velocities in the transversal direction were much higher than longitudinal velocities, both on the base and the top of the piers. Vertical velocities at the pile cap were of the same order as the longitudinal ones. The already observed resonance frequencies were found. Records relative to sensors in longitudinal direction were always in phase at the selected resonance frequencies. As a result, one can state that no torsional modes are associated with these frequencies. In Figs. 18 and 19, the cross-spectra of records in transversal direction are plotted for pier 2 and pier 3, respectively.

5 The finite element model

The experimental results were compared with those obtained from a finite element model set-up using Midas code (Fig. 20). The structural elements were considered in their non-damaged condition.

The columns of each pier were modeled as beams, fully fixed at the pier base and linked to each other at their top and connected to the pier cap. The deck was modeled as

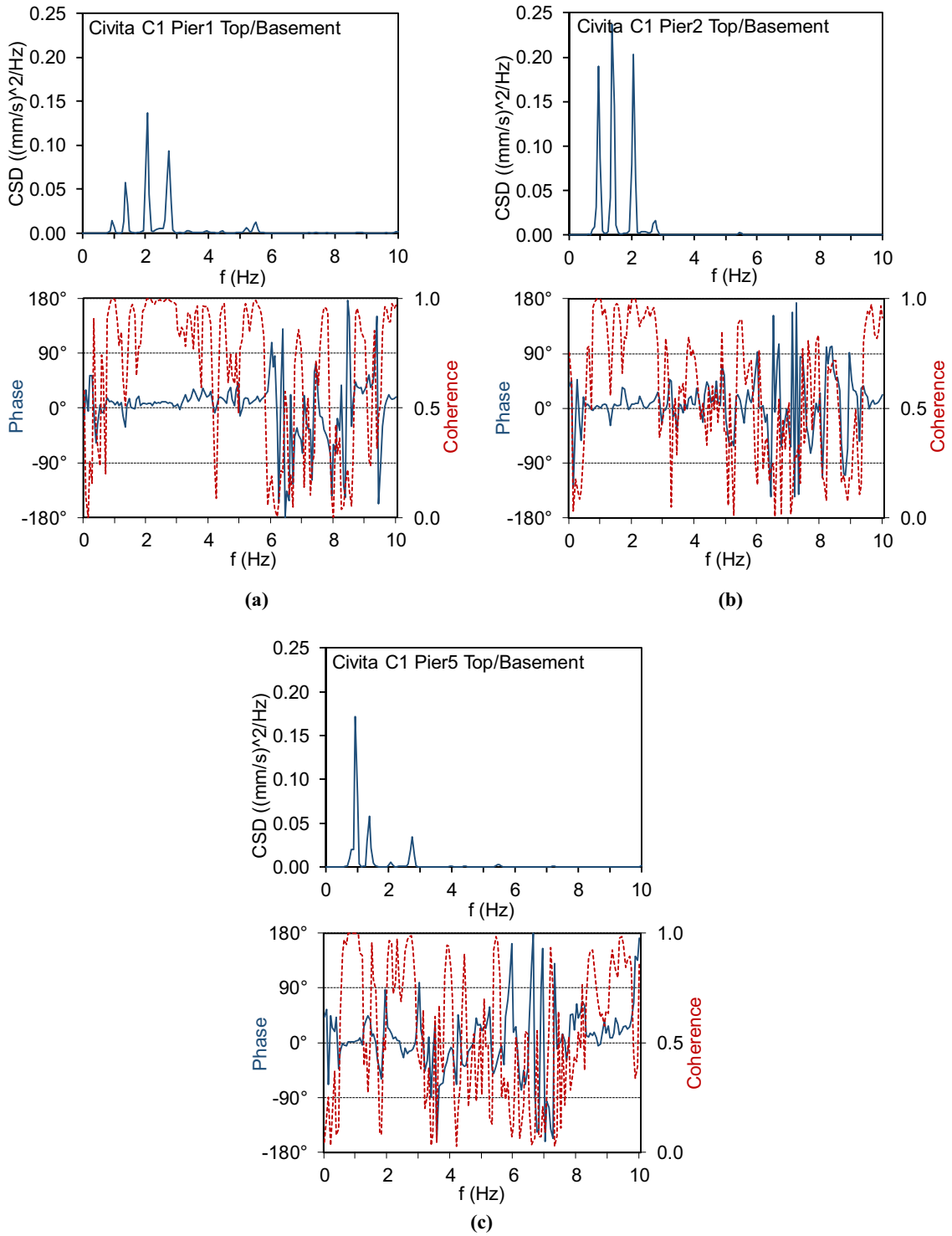

Fig. 14 CSDs of recordings at the top and the basement of **a** pier 1, **b** pier 2 and **c** pier 5, in the transversal direction, under forced vibrations

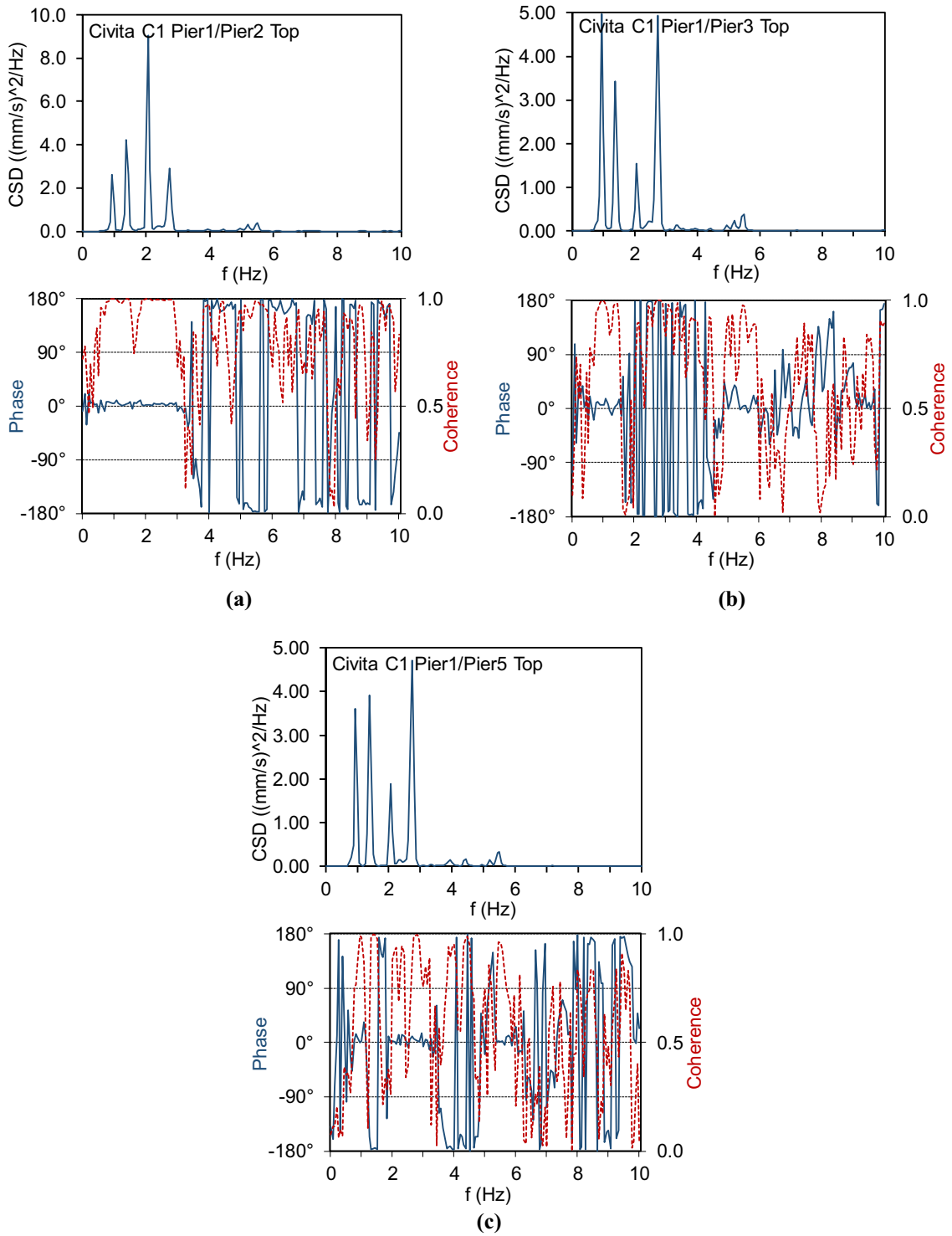

Fig. 15 CSDs of recordings at **a** the tops of pier 1 and pier5, **b** pier 1 and pier 3 and **c** pier 1 and pier 5, in the transversal direction, under forced vibrations

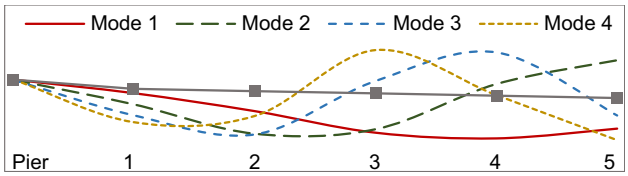

Fig. 16 Experimental normalized modal shapes in the transversal direction

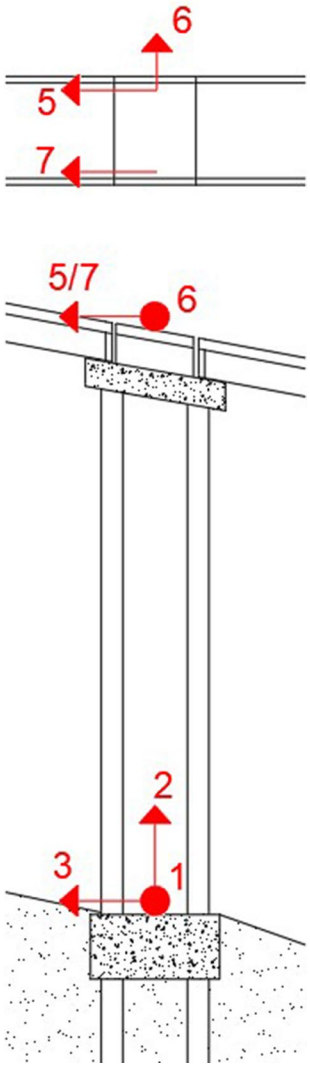

Fig. 17 Sensor deployments to analyze the behavior of the single piers

a beam having its geometrical and mechanical properties. The interaction between the deck and the pier was realized by means of the structural system in Fig. 21, where

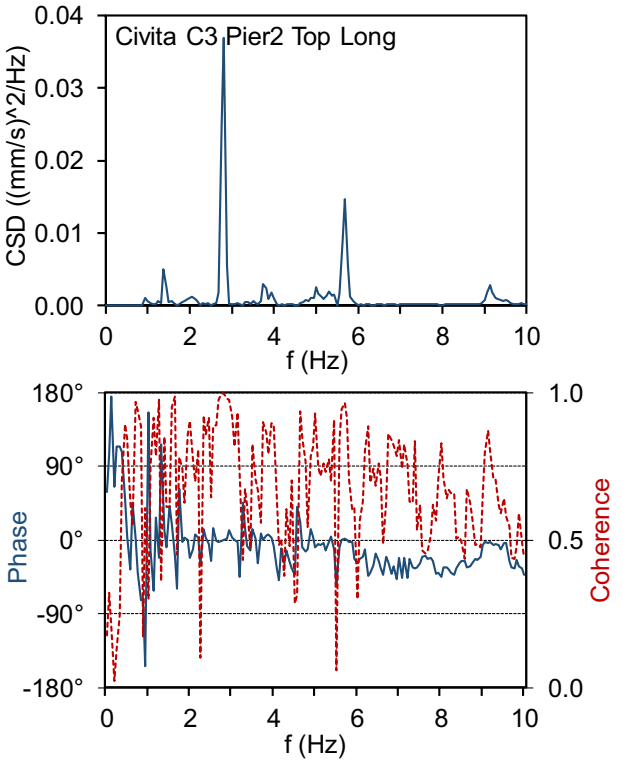

Fig. 18 CSDs of recordings in the longitudinal direction at the top of pier 2

rigid beams (thick lines) were considered to simulate the presence of three bearings under the three beams. The lead bearings were assumed rigid in the vertical direction but characterized by a finite stiffness in the horizontal directions ($K_h = 10^4$ kN/mm), which was derived from the typical characteristics of the lead.

The deck is subject to its self-weight (17.5 kN/m and 6.3 kN for each transverse beam for the 3-beam deck, 28.25 kN/m and 6.8 kN for each transverse beam for the 5-beam deck of the first span) and to the permanent loads, i.e., the pavement (2.00 kN/m^2) and the metal banisters and the concrete curb (1.45 kN/m).

The Young's modulus of piers and decks was deduced from the concrete strengths (see Table 4) and then adjusted to obtain the coincidence between the first experimental and numerical resonance frequencies. Finally, the values of 31,000 and 35,000 N/mm^2 were assumed for the piers and the decks, respectively.

The modal analysis gave the first four modal shapes in the transversal direction, plotted in Fig. 22. These are very similar to the experimental ones; the resonance frequencies, instead, are a bit higher (Table 7). This occurrence

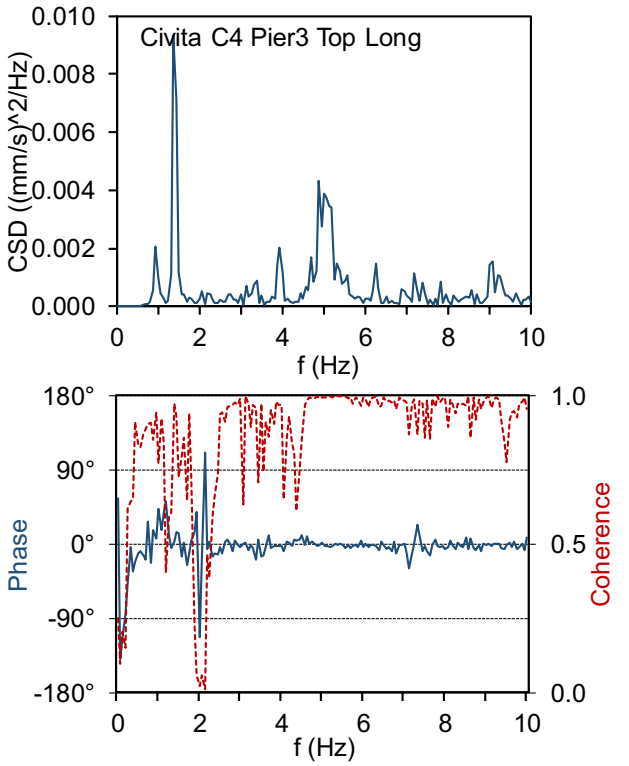

Fig. 19 CSDs of recordings in the longitudinal direction at the top of pier 3

demonstrated that the actual stiffness of the piers is lower than the original ones, relative to the undamaged structure, but the stiffness decrease was almost uniformly distributed along the spans and not present only in one or few elements.

The seismic vulnerability analysis was carried out assuming a behavior factor equal to 1. Pier 10 reaches first its ultimate limit state firstly by yielding the sections at the column feet, with a ground acceleration of 0.092 g, which

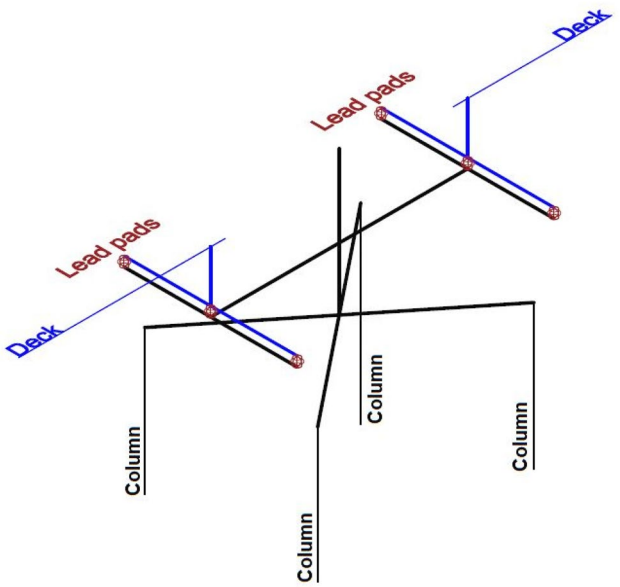

Fig. 21 Modeling of the interaction between the decks and the pier

corresponds to an earthquake at the site with an exceedance probability of about 30% in 50 years.

6 Conclusions

The structural evaluation of the pedestrian bridge accessing Civita di Bagnoregio, carried out according to the Italian LG2020, pointed out a high Class of Attention, which requires a detailed study based on experimental analyses. These were done with particular focus on:

– Laboratory analyses on disturbed and undisturbed samples, in situ cone penetration tests (CPT) and standard dynamic tests (DPHS) on the subsoil.

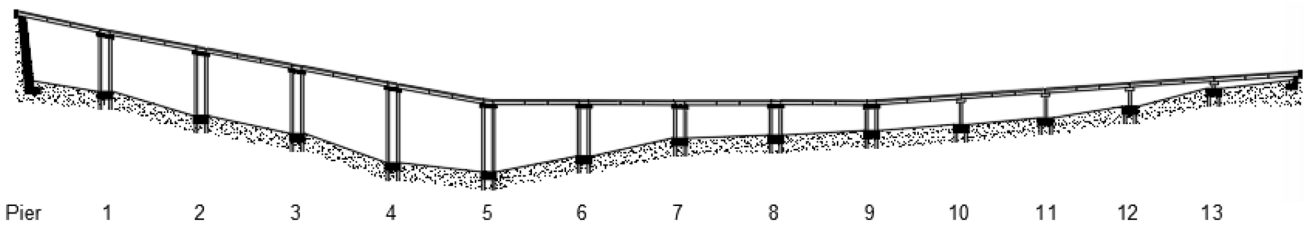

Fig. 20 Schematic view of the bridge

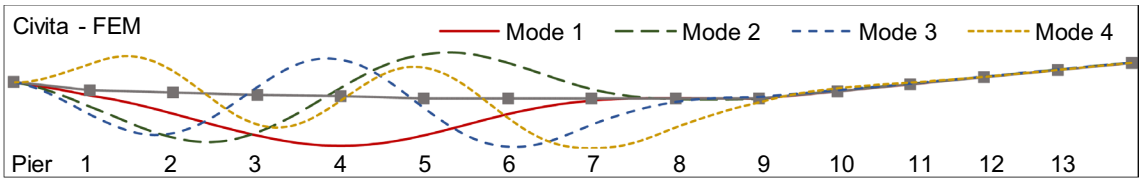

Fig. 22 Normalized modal shapes in the transversal direction from numerical model

- Pull-out tests, ultrasonic tests, sclerometer tests and carbonation tests on the beams, piers and foundation plinths.
- Laboratory tests on the concrete, i.e., compression strength tests, and on the reinforcing steel bars, i.e., tension strength tests.
- Experimental vibration analysis, using ambient vibrations and forced vibrations induced by the passage of vehicles and/or people.

The outcomes confirmed the excellent quality and homogeneity of the clay soil and the concrete of all the structural elements. The girder showed a linear elastic behavior under increasing static loading. The experimental deflections resulted lower than the theoretical ones.

The experimental vibration analysis allowed to state that the structural behavior of the bridge was quite similar to the expected one, i.e., to the structural behavior predictable from theory and/or from numerical simulations or from what observed on the field for similar bridge typologies, from a qualitative point of view. Under ambient vibrations, the structure composed of piers linked at their tops by means of the decks, behaved as a whole. No unpredictable behaviors of one particular pier in comparison to the others or proof of bad conditions of the foundation structures were detected.

The structure showed very high deformability, more evident in the proximity of the highest piers due to the slenderness of the vertical elements; the deformability was emphasized by the observed defects and damage, which resulted in a reduction of the effective cross sections of the pier columns.

The experimental analyses were carried out to collect the information needed for an accurate evaluation. The mathematical model, based on a detailed survey and experimental data, showed quite good results, in terms of dynamic behavior under ambient vibrations, while the seismic vulnerability resulted very high. Considering the importance of the bridge, which is the only way to access the "dying town", a permanent monitoring system would be advisable to inform, though structural health monitoring data and evidences, a maintenance on request and preventive maintenance campaign that could contain maintenance cost while guarantying the safety of the access to Civita di Bagnoregio.

Acknowledgements The study described in this paper is part of the activities of ENEA and Consorzio Civita in the field experimental laboratory at Civita di Bagnoregio. The authors acknowledge Dr. Claudio Margottini, coordinator of the project.

Funding Open access funding provided by Ente per le Nuove Tecnologie, l'Energia e l'Ambiente within the CRUI-CARE Agreement.

References

1. Buratti G, Cosentino A, Morelli F, Salvatore W, Bencivenga P, Zizi M, De Matteis G (2019) Alcune considerazioni sull'evoluzione normativa dei carichi da traffico nella progettazione dei ponti stradali in Italia. XVII Convegno ANIDIS, Ascoli Piceno, 15–19(SS05). Sept 2019:2–16 (**In Italian**)
2. Frangopol D, Bocchini P (2011) Bridge network performance, maintenance and optimisation under uncertainty: accomplishments and challenges. Structure and Infrastructure Engineering 8(4). https://doi.org/10.1080/15732479.2011.563089.
3. Jeong Y, Kim WS, Lee I, Lee J (2018) Bridge inspection practices and bridge management programs in China, Japan, Korea and U.S. Journal of Structural Integrity and Maintanance, 3(2). https://doi.org/10.1080/24705314.2018.1461548.
4. Honfi D, Bjirnsson I, Ivanov OL, Leander J (2020) Informed successive condition assessments in bridge maintenance. J Civil Structural Health Monitoring 10:729–737. https://doi.org/10.1007/s13349-020-00415-2
5. Circolare Min. LL.PP. 6736/61A1 del 19.07.1967: "Controllo delle condizioni di stabilità delle opere d'arte stradali".
6. Ordinanza del Presidente del Consiglio dei ministri 20 marzo 2003, n. 3274. G.U. n. 105 del 8 maggio 2003. n.72.
7. MIT: NTC-2008 Nuove Norme tecniche per le costruzioni. Gazzetta Ufficiale Serie Generale n.29 del 04–02–2008 - Suppl. Ordinario n. 30.
8. MIT: NTC-2018 Aggiornamento delle Norme tecniche per le costruzioni. Supplemento ordinario alla Gazzetta Ufficiale, No. 42 of February 20, 2018 - Serie generale (2018).

9. MIT (2020) Linee guida per la classificazione e gestione del rischio, la valutazione della sicurezza ed il monitoraggio dei ponti esistenti. Ministero delle Infrastrutture e dei trasporti.
10. Phares BM, Rolander DD, Graybeal BA, Washer GA (2001) Reliability of Visual Bridge Inspection. Public Roads, Federal Highway Administration Research and Technology, 64(5).
11. Agrawal AK, Washer G, Alampalli S et al (2021) Evaluation of the consistency of bridge inspection quality in New York State. J Civ Struct Health Monitoring 11:1393–1413. https://doi.org/10.1007/s13349-021-00517-5
12. Clemente P, De Stefano A (2016) Novel methods in SHM and monitoring of bridges. Foreword. Special Issue of J. of Civil Structural Health Monitoring 6(3), Springer. https://doi.org/10.1007/s13349-016-0185-4.
13. Clemente P, Bongiovanni G, Buffarini G, Saitta F (2019) Structural health status assessment of a cable-stayed bridge by means of experimental vibration analysis. J. of Civil Structural Health Monitoring 9(5), 655–669, Springer. https://doi.org/10.1007/s13349-019-00359-2.
14. Clemente P (2020) Monitoring and evaluation of bridges. Lessons from the Polcevera Viaduct collapse in Italy. J. Civil Structural Health Monitoring, 10(2), 177–182, Springer. https://doi.org/10.1007/s13349-020-00384-6.
15. Bongiovanni G, Cellilli A, Clemente P, Giovinazzi S, Ormando C (2021) Seismic response of a r.c. viaduct during different earthquakes. In: Cunha A., Caetano E. (eds), Proc. 10th Int. Conf. on Structural Health Monitoring of Intelligent Infrastructure (SHMII-10, 30 June – 2 July 2021, Porto), ABS_247.
16. Chun-Xu Qu, Yi T-H, Li H-N, Chen B (2018) Closely spaced modes identification through modified frequency domain decomposition. Measurement 128:388–392
17. Chun-Xu Qu; Ting-Hua Yi, A.M. (2018) ASCE; Yu-Zheng Zhou; Hong-Nan Li. Frequency identification of practical bridges through higher order spectrum. Journal of Aerospace Engineering, ASCE, 31(3): 04018018. https://doi.org/10.1061/(ASCE)AS.1943-5525.0000840.
18. Chun-Xu Qu; Ting-Hua Yi, Hong-Nan Li. Mode identification by eigensystem realization algorithm through virtual frequency response function, Structural Control and Health Monitoring, 2019, 26(10): e2429. https://doi.org/10.1002/stc.2429
19. Sun Z, Sun H (2018) Jiangyin Bridge: An Example of Integrating Structural Health Monitoring with Bridge Maintenance. Struct Eng Int 2018(28):353–356. https://doi.org/10.1080/15732479.2017.1360365
20. Bas S, Apaydin NM. Ilki A. Catbas FN (2018). Structural health monitoring system of the long-span bridges in Turkey. Struct. Infrastruct. Eng. 2018, 14, 425–444. https://doi.org/10.1080/15732479.2017.1360365
21. Wong K.Y (2004). Instrumentation and health monitoring of cable-supported bridges. Structural Control and Health Monitoring. Vol. 11, Issue 2. https://doi.org/10.1080/15732479.2017.1360365.
22. Gentile C, Saisi A (2015) Continuous dynamic monitoring of a centenary iron bridge for structural modification assessment. Front Struct Civ Eng 2015(9):26–41. https://doi.org/10.1007/s11709-014-0284-4
23. Norouzzadeh Tochaei E, Fang Z, Taylor T, Babanajad S, Ansari F (2021) Structural monitoring and remaining fatigue life estimation of typical welded crack details in the Manhattan Bridge. Eng Struct 2021(231):111760. https://doi.org/10.1016/j.engstruct.2020.111760
24. Chiaia B, Marasco G, Ventura G et al. (2020) Customised active monitoring system for structural control and maintenance optimisation. J Civil Struct Health Monit 10, 267–282, Springer. https://doi.org/10.1007/s13349-020-00382-8.
25. Kwon T, Park S, Park S et al (2021) Building information modeling-based bridge health monitoring for anomaly detection under complex loading conditions using artificial neural networks. J Civil Struct Health Monit 11:1301–1319. https://doi.org/10.1007/s13349-021-00508-6
26. Zhelyazkov A, Zonta D, Wenzel H et al (2020) On the estimation of the ductility demand on reinforced concrete bridge piers from structural health monitoring data. J Civil Struct Health Monit 10:283–329. https://doi.org/10.1007/s13349-020-00383-7
27. Enckell M, Glisic B, Myrvoll F et al (2011) Evaluation of a large-scale bridge strain, temperature and crack monitoring with distributed fibre optic sensors. J Civil Struct Health Monit 1:37–46. https://doi.org/10.1007/s13349-011-0004-x
28. Lorenzoni F, De Conto N, da Porto F et al (2019) Ambient and free-vibration tests to improve the quantification and estimation of modal parameters in existing bridges. J Civil Struct Health Monit 9:617–637. https://doi.org/10.1007/s13349-019-00357-4
29. Zarafshan A, Ansari F, Taylor T (2014) Field tests and verification of damping calculation methods for operating highway bridges. J Civil Struct Health Monit 4:99–105. https://doi.org/10.1007/s13349-013-0067-y
30. Kariyawasam KD, Middleton CR, Madabhushi G et al (2020) Assessment of bridge natural frequency as an indicator of scour using centrifuge modelling. J Civil Struct Health Monit 10:861–881. https://doi.org/10.1007/s13349-020-00420-5
31. Ormando C, Raeisi F, Clemente P, Mufti A (2022) The SHM as higher level inspection in the evaluation of structures. In: Pellegrino C. et al. (eds) Proc. of the 1st Conference of the European Association on Quality Control of Bridges and Structures (EUROSTRUCT, Padua 29 Aug—1 Sep 2021), Lecture Notes in Civil Engineering, 200, 452–461, Springer, Cham. https://doi.org/10.1007/978-3-030-91877-4_52.
32. Ormando C, Ianniruberto U, Clemente P, Giovinazzi S, Pollino M, Rosato V (2021) Real-time assessment of performance indicators for bridges to support road network management in the aftermaths of earthquake events. In Papadrakakis M, Fragiadakis M (eds.), Proc. of the 8th ECCOMAS Thematic Conference on Computational Methods in Structural Dynamics and Earthquake Engineering (COMPDYN 2021, 27–30 June 2021, Streamed from Athens, Greece), 2, 3536–3550, National Technical University of Athens. ISBN(set): 978–618–85072–5–8, ISBN(vol II): 978–618–85072–4–1. https://doi.org/10.7712/120121.8728.19414.
33. Buffarini G, Clemente P, Giovinazzi S, Ormando C, Pollino M, Rosato V (2022). Preventing and Managing Risks induced by Natural Hazards to Critical Infrastructures. Infrastructures 2022, 7(6), 76, MDPI Basel, Switzerland. https://doi.org/10.3390/infrastructures7060076.
34. Blaso L, Clemente P, Giovinazzi S, Giuliani G, Gozo N, Ormando C, Pollino M, Rosato V (2022) Towards Standardized and Interoperable Platforms for supporting the Seismic Vulnerability Assessment and Seismic Monitoring of Italian Bridges and Viaducts". In: Pellegrino C. et al. (eds) Proc. of the 1st Conference of the European Association on Quality Control of Bridges and Structures (EUROSTRUCT, Padua 29 Aug—1 Sep 2021), Lecture Notes in Civil Engineering, Vol 200, 471–480.

Springer, Cham, online 12 Dec 2021. https://doi.org/10.1007/978-3-030-91877-4_54.
35. Focardi P, Margottini C, Ogliotti C, Sciotti M, Serafini S (1998) Civita di Bagnoregio: the dying town. Proc. of the X ECSMEF (Florence), AGI, Roma.
36. Margottini C, Serafini S (eds) (1990) Civita di Bagnoregio. Osservazioni geologiche e monitoraggio storico dell'ambiente. Una ricerca ENEA. Associazione Progetto Civita, Roma (**in Italian**)
37. SGM Engineering (1997) Indagini sperimentali sul viadotto di accesso a Civita di Bagnoregio. Report to Bagnoregio Town and Annexes, (**in Italian**).